Laser Physics, Vol. 10, No. 6, 2000, pp. 1188–1207.

Photodynamic Therapy and Fluorescence Diagnostics

V. B. Loschenov, V. I. Konov, and A. M. Prokhorov

Center of Natural Research, General Physics Institute, Russian Academy of Sciences, ul. Vavilova 38, Moscow, 117942 Russia

e-mail: biospec@mail.ru

Abstract—We present the results of research and development in photodynamic therapy and fluorescence diagnostics performed by the Center of Natural Research, General Physics Institute, Russian Academy of Sciences, in collaboration with several research and medical institutes. The main attention is focused on physical aspects of the problem. We describe schemes and the principle of operation of devices employed by our group in clinical and experimental studies. The problems of interaction of laser radiation with biological tissues are considered. The assessment of an outlook for using different photosensitizers is based on their spectral–fluorescent properties, their ability to excite molecular oxygen, and their stability to irradiation with light. Some results of clinical applications of the developed devices and methods are presented.

INTRODUCTION

Methods of photodynamic therapy (PDT) and fluorescence diagnostics (FD) have been considered in numerous studies in many different countries, including Russia [1–15]. An interest in this field of research is associated with broad opportunities of applying PDT and FD methods in a diagnosis and treatment of oncological diseases. Some promising results have been also recently obtained in other areas of medicine, such as vascular diseases, skin diseases, and some infectious diseases, including tuberculosis.

Research in this direction was started at General Physics Institute ten years ago [16]. Investigations were carried out in collaboration with prominent medical centers, including Moscow Medical Academy, Oncological Research Center, Herzen Institute, Institute of Laser Medicine, etc. These studies were considerably stimulated by the advent of Russian photosensitizers, produced by the Research Institute of Organic Polymers and Dyes Russian Federation State Research Center and the Institute of Fine Chemical Technologies.

A series of laser and spectroscopic instruments developed by the Center of Natural Research, General Physics Institute, Russian Academy of Sciences, are currently successfully used in many clinics in Moscow and several clinics in Russia and abroad.

Although these methods have received a broad acceptance, their potential is far from being exhausted. In this paper, we propose possible ways of developing these methods with allowance for the progress that has been already achieved. Some excessive use of medical terminology, which is not characteristic of a physical journal, is due to the specific nature of these methods and the area where these methods are applied.

Photodynamic Therapy and Fluorescence Diagnostics

The term photodynamic therapy was introduced to denote the effect of light action on a biological tissue. The presence of a photosensitizer (PS) in a biological tissue is the necessary condition of the photodynamic effect. The properties of this photosensitizer determine to a large extent the efficiency of photodynamic treatment. Photosensitizers based on the so-called oxygen mechanism are characterized by the highest efficiency among the available photosensitizers. In practice, this implies that the energy of absorbed photons is partially spent on fluorescence and partially transferred to molecular oxygen through a metastable triplet state. Oxygen under these conditions is transferred to an excited singlet state, which is characterized by a high oxidation activity. Therefore, if some cell or bacterium contains a PS and oxygen, then light with a wavelength corresponding to PS absorption destroys biological macromolecules. As the concentration of a PS and oxygen in cells or bacteria reaches some critical level, these cells or bacteria die (Fig. 1).

Since the energy of absorbed photons is partially emitted in the form of fluorescence, it would be natural to detect this radiation in order to determine the PS concentration in a biological tissue and to monitor the dynamics of this irradiated tissue in the time domain. This concept provides a background for FD. Thus, three conditions are necessary for successful FD and PDT:

(1) A pathologic cell should "want" to absorb a PS. We have to force this cell to do it otherwise;

(2) A sufficient amount of molecular oxygen in the neighborhood of a PS is necessary to ensure a high efficiency of this PS;

(3) The number of photons should be sufficient to trigger the reaction leading to the death of a cell or biological tissue, but should not exceed the level corresponding to the death of a cell due to the thermal effect, although such an effect may be positive in certain cases.

The main purpose of our research in this very broad area is not only to measure the parameters specified above, but also to control these parameters. An important requirement in such experiments is that the methods and equipment should be adapted to clinical conditions.

The main advantage of methods of *in vivo* spectral analysis of tissues is associated with the noninvasive character of this approach, which allows one to obtain the information concerning the state of tissues without influencing the dynamics of different biological processes. Such an intervention may often be undesirable and even dangerous. For example, biopsy tissue sampling from a melanoma may lead to a generalization of a tumor formation process.

Another advantage of optical analysis of tissues is associated with the possibility of real-time data processing and correction of parameters of a therapeutic process in accordance with the information thus obtained. Specifically, analysis of the concentration and the chemical state of photosensitizers in the PDT process provides an opportunity to correct the intensity of laser radiation.

We should note also that, due to the progress achieved in optoelectronics and microprocessor engineering, a system for spectral analysis of tissues can be made compact and portable.

EQUIPMENT

The hardware for PDT and FD should comply with the following requirements.

Performance

The rate of renewing the measured spectrum or a fluorescence image should not exceed 0.5–1 s. In our studies, this quantity is typically around 100 ms, which is sufficient to avoid errors due to heart pulses, peristalsis, breathing, or nerve pulses. Data processing in these measurements is performed in real time, which makes it possible to estimate the PS concentration or the oxygenation degree of hemoglobin in tissues being studied and to make a decision promptly. The total time that can be spent on a fluorescence diagnostics of a stomach, lung, or some other hollow organ never exceeds 1–2 min. The time that can be spent on PDT ranges from 10–15 min for hollow organs up to an hour for skin. The power density of radiation is chosen in such a way as to meet these requirements.

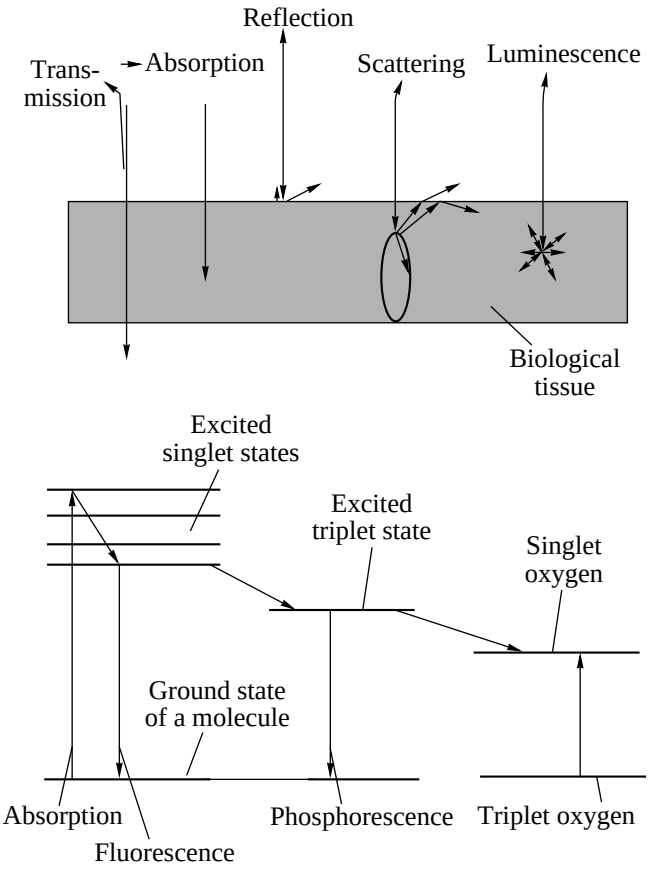

Fig. 1. Interaction of light with biological tissues in the case of fluorescence diagnostics and photodynamic therapy.

Precision

The precision of biological measurements is usually not very high, and the scatter in PS concentrations for the same dose administered into different patients may vary by a factor of 1.5–2 in the case of the same biological tissue. Therefore, the precision of concentration determination allows a scatter of 20–30%. The precision of oxygenation degree determination should not exceed 8–10%. The uniformity of intensity distribution in a light beam in the course of therapy should not exceed 15–20%. The precision of determining the radiation dose absorbed by a biological tissue should be no lower than 20–30%.

Sensitivity

The concentration of photosensitizers ranges during FD and PDT on the average from 0.1 to 10 mg per kilogram of patient's weight. We achieved a high sensitivity in our studies [17–19] due to the use of a special fiber-optic device shown in Fig. 2. Laser radiation with an intensity of 10 mW is delivered along the central fiber. Since the fiber diameter is 200 μm, the power density is

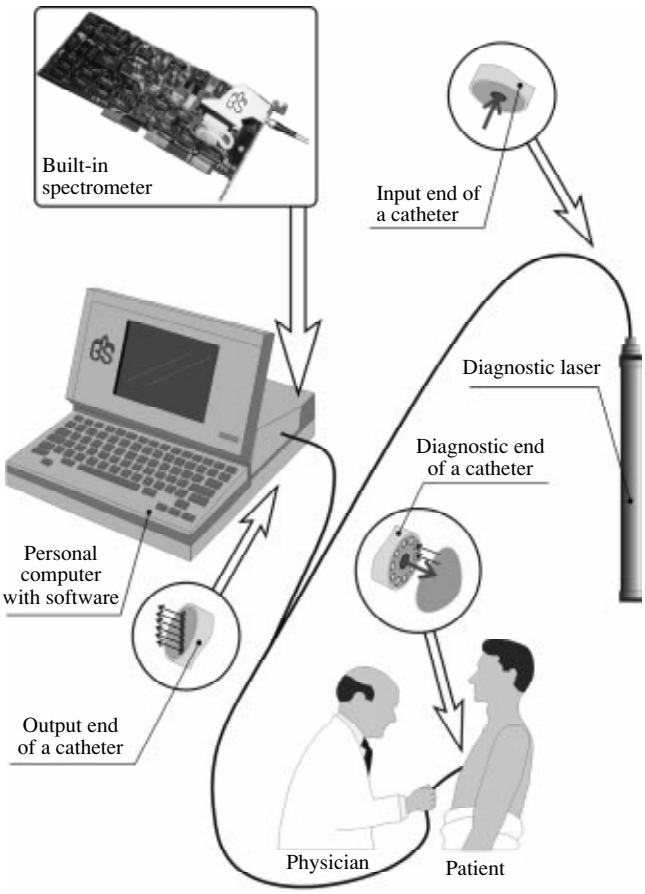

Fig. 2. Diagram of a portable system for measuring fluorescence and reflection spectra of tissues *in vivo*.

rather high (30 W per square centimeter). Thus, the density of radiation used for diagnostics varies, depending on the fiber diameter, from several up to 50 W per square centimeter. In spite of such a high power density, radiation causes no pain as it comes in contact with a tissue. This radiation power is mainly scattered within a 2-mm^3 volume of a biological tissue. Correspondingly, the information concerning the PS concentration in a biological tissue can be obtained from the same volume. A high sensitivity in the determination of the oxygenation degree is achieved due to the increase in the distance between the light coming into a biological tissue and the light going out of this tissue. Thus, the number of centers involved in the absorption of light scattered inside a tissue increases. Usually, the distances of 1 to 10 mm are used, depending on the blood-filling factor of the organ under study. Another solution of this problem is to employ a broad illuminating beam. To record spectra of backward scattering, we employ miniature halogen incandescent lamps with an elliptic reflector with a power of 10–20 W as sources of light. In endoscopic studies, a standard endoscope condenser was used as a source of light, while the optical channel of an endoscope served as a fiber-optic catheter.

In what follows, we will consider the principle of operation and some design features of several devices developed at the Center of Natural Research, General Physics Institute, Russian Academy of Sciences, and employed in clinical practice.

A LESA-6 LASER–ENDOSCOPIC SPECTRUM ANALYZER

A diagram of the developed portable spectroscopic system is presented in Fig. 2. The light produced by a laser source or a lamp built in the extension station of a Notebook computer is focused on the output end of a Y fiber-optic catheter. Radiation is delivered to a distance of several centimeters from the full contact with a tissue (depending on the character of the problem being solved). The distal end of the catheter is designed in such a way that it can be inserted into the biopsy channel of a usual endoscope for studying inner organs or into a tip for intratissue analysis. Fluorescence and scattered light passes through the receiving fibers, which surround the light-delivering fiber. Variations in the distance between the catheter and a tissue within the range from 0 to 2 cm and the tilt angle from 0° to 30° give rise to errors in the determination of the PS concentration not exceeding 10%. Fibers are arranged in a series at the output end of the catheter, which is connected to a spectrograph, in such a way that the light flux is increased without any losses in the resolution. A narrow-band optical filter, reducing the intensity of backward-scattered laser light by a factor of 10000, is placed in front of the entrance of the spectrograph. This scheme allows the spectra of fluorescence and backward-scattered laser radiation to be analyzed on the same scale. This approach permitted the normalization of spectra, the quantitative estimation of PS concentration in different tissues, and comparison of the results obtained at different times with different instruments. A spectrograph with electronic units for data acquisition was assembled on a computer board, which can be inserted into an ISA slot of the extension station of a Notebook computer. The detected signal is digitized, inputted into computer memory, and displayed on a computer screen in real time [Patents 1–3].

Such a relatively simple system allows the spectrum of diffuse reflection and fluorescence to be recorded with a repetition rate of 0.1 s, which is sufficient for real-time monitoring. This system can also perform many functions due to a special software, operating under Windows. Different standard samples were developed to ensure a high efficiency of this system for biomedical and clinical applications. The scattering coefficients and PS concentrations in these samples were chosen at the level typical of organs and tissues subject to PDT. Different lasers producing radiation with wavelengths ranging from the ultraviolet to the infrared region were employed to excite fluorescence.

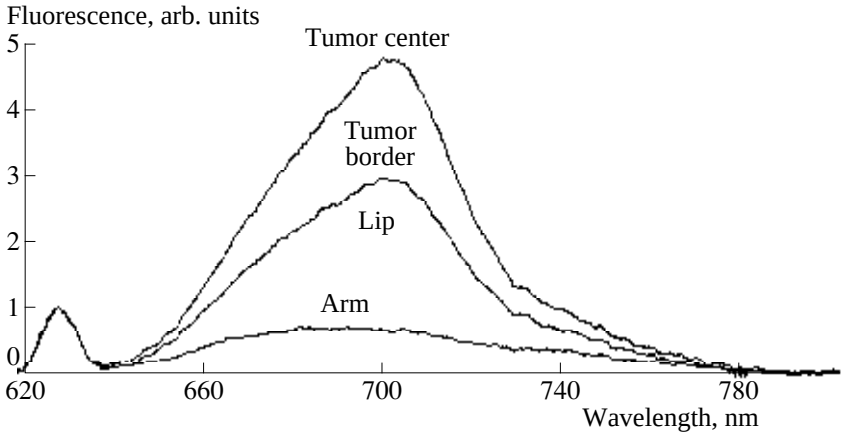

Fig. 3. Fluorescence spectra of tumorous and normal tissues with a Photogem photosensitizer (2 mg/kg, 24 h after the injection).

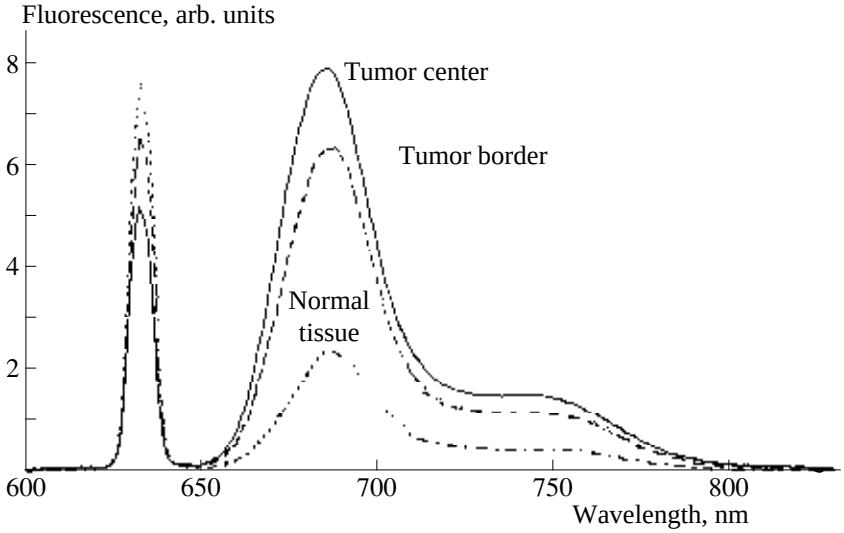

Fig. 4. Fluorescence spectra of tumorous and normal tissues with a Photosense photosensitizer (0.5 mg/kg, 24 h after the injection).

A helium–neon laser provided the best set of parameters for the excitation of fluorescence in photosensitizers employed in clinical studies. Advantages of a helium–neon laser include the stability of radiation wavelength, the absence of long-wavelength tails (which is a problem in the case of laser diodes), and a much larger depth of penetration into a tissue as compared with other lasers in the visible and ultraviolet ranges. In addition, the fluorescence quantum yield is highly sensitive to variations in the blood-filling factor of an organ under study, which has an influence on the stability and the reliability of the results of diagnostics.

Typical fluorescence spectra of a tumor containing a photosensitizer are presented in Figs. 3–5 [19]. These spectra were recorded during the photodynamic therapy of skin tumors. Figure 3 displays the spectra of tumorous and normal tissues containing a Photogem photosensitizer (a photosensitizer of the first generation) recorded 24 h after the intravenous injection of a 2-mg/kg dose of the preparation. The peak of fluorescence at the wavelength of 698 nm is associated with the contribution of the photosensitizer. Note that the natural fluorescence of tissues also provides a contribution within this spectral range, which should be taken into consideration for the correct estimation of the PS concentration in tissues. Figure 4 presents the spectra of a cheek tumor recorded in experiments where sulfonated aluminum phthalocyanine (Photosense, a photosensitizer of the second generation) was employed as a photosensitizer. These spectra were measured 24 h after the systematic injection of a 0.5-mg/kg dose of the preparation. The contrast of photosensitizer accumulation (the ratio of PS concentrations for tumorous and normal tissues) determined from these spectra was equal to 2.5. The extinction coefficient and the fluorescence quantum yield for Photosense are much higher than the corresponding parameters for Photogem. Therefore, the contribution of natural tissue fluorescence is negligible in this case as compared with the PS contribution.

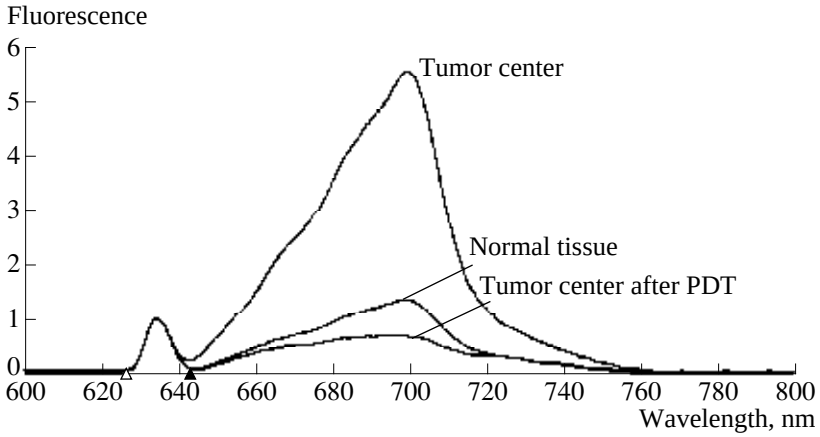

Fig. 5. Fluorescence spectra of a stomach tumor and a normal stomach tissue 3 h after the peroral injection of 300 mg of 5-ALA. The spectrum of a tumor after laser irradiation in the process of PDT, showing complete photobleaching, is also presented.

Figure 5 presents fluorescence spectra for a malignant tumor of stomach and a normal stomach tissue recorded 3 h after the peroral injection of 5-amino levulinic acid (5-ALA) (the dose was 5 mg per kilogram of patient's weight). Note that ALA itself does not fluoresce, but it triggers the mechanism of porphyrin formation in a cell, eventually leading to heme formation. Healthy cells recycle more excessive ALA than tumorous cells. As a result, tumorous cells accumulate excessive amounts of one of porphyrins—protoporphyrin IX, which displays a high-intensity fluorescence and features a sufficiently strong photodynamic effect. The fluorescence spectrum of ALA-induced protoporphyrin IX differs from the spectrum of natural fluorescence by a red shift of the intensity maximum in the spectrum. The fluorescence intensity decreases after laser irradiation down to the level characteristic of natural fluorescence due to photobleaching. The bleaching of protoporphyrin IX in the specific case under study was induced by a radiation dose small as compared with the radiation dose inducing the photobleaching of, for example, Photosense.

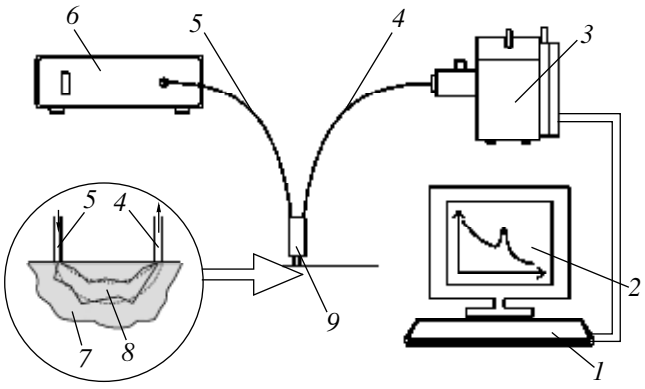

Fig. 6. (*1*) Personal computer, (*2*) absorption spectrum, (*3*) LESA-01-UL-BIOSPEC laboratory laser electron–spectral universal setup, (*4*) receiving fiber-optic catheter, (*5*) irradiating fiber-optic catheter, (*7*) biological tissue, (*8*) area of measurements, and (*9*) holder of fiber-optic catheters.

A LESA-01-UL-BIOSPEC UNIVERSAL SPECTRUM ANALYZER

Diagram of the experimental system is shown in Fig. 6. White light produced by a halogen lamp source was coupled into a quartz fiber and delivered to a tissue. The light diffuse-scattered by the tissue was collected with receiving fibers and entered into a spectrometer. The spectrometer was controlled by a computer with the use of a special computer code working under Windows. Absorption spectra of an object under study (not corrected for scattering) were displayed on a computer screen in real time. The oxygenation degree of hemoglobin was calculated from the analysis of absorption spectra in the visible range. The dynamics of this parameter was also displayed on a computer screen in real time. The relative error of oxygenation-degree calculations was less than 3%, while the absolute error was less than 10%. The size of the probing area ranged from 1 to 2 mm, thus including the contribution of many capillaries [20].

The presence of molecular oxygen in tissues is especially important for photosensitizers using the singlet oxygen generation mechanism (II type). It is well known that tumorous tissues often reside in a hypoxia state, and the deficiency of molecular oxygen may be a limiting factor in chains of photochemical reactions leading to the death of cancer cells in the course of PDT.

We have developed a sufficiently precise and reliable technique [Patent 4] and the corresponding hardware for measuring the oxygenation degree of hemoglobin in tissues in the course of PDT from absorption or backward-scattering spectra of these tissues. Hemoglobin, water, lipids, and melanin are the main chromophores of normal tissues in the visible spectral

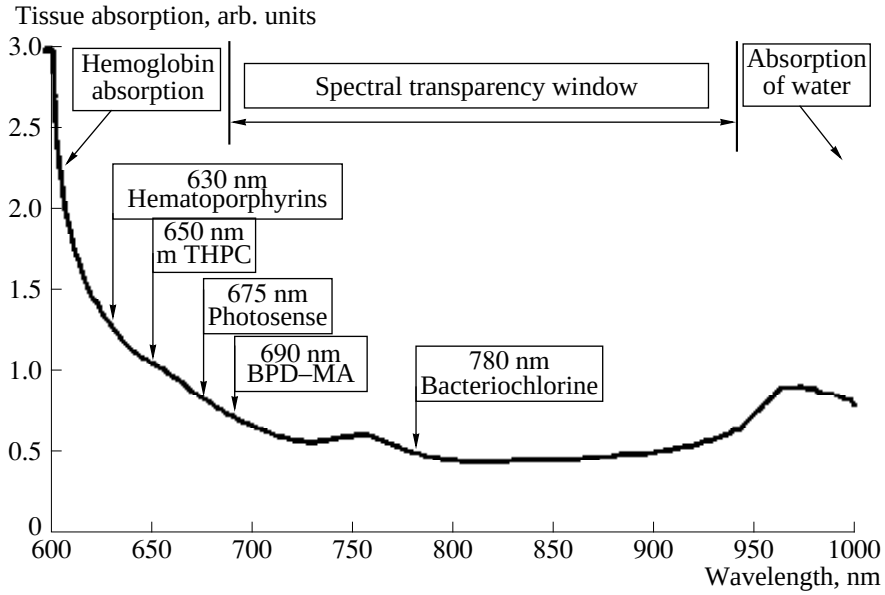

Fig. 7. Dependence of the absorption coefficient of a tissue (without corrections for scattering), demonstrating the therapeutic transparency window of tissues within the range of 650–1000 nm. Absorption maxima of the main photosensitizers employed for PDT are also shown.

range. Photosensitizers employed for PDT (especially, photosensitizers of the second generation) may also provide a considerable contribution to the absorption of tissues. The maximum optical transparency of biological tissues is achieved within the range from 650 to 1000 nm (Fig. 7). Photons with shorter wavelengths are efficiently absorbed by blood hemoglobin, while photons with longer wavelengths are absorbed by water. The data on absorption spectra of tissues are very important for PDT, as they can provide the following information. First, the contribution due to PS absorption can be separated in absorption spectra of tissues, which allows the PS concentration and state to be assessed (Fig. 8). It is well known that, due to their high extinction coefficient, photosensitizers of the second generation may considerable decrease the penetration depth of light in a tissue (the screening effect), which should be taken into consideration when one estimates the optimal concentration of a PS for therapy. In particular, when high concentrations of Photosense are used, the penetration depth at the wavelength of 675 nm (the wavelength employed for therapy) may become comparable with the penetration depth of a tissue at the wavelength of 630 nm. In other words, because of the screening effect, we may lose the advantages of this photosensitizer for the therapy of deep tissue layers.

Second, by analyzing absorption spectra in the visible range, we can estimate the oxygenation degree of blood hemoglobin. This parameter is very important for PDT. On the one hand, it reflects the rate of oxygen consumption in tissues, thus, giving an idea of the intensity of photodynamic reactions. On the other hand, this parameter characterizes the destruction degree of a capillary alveus in the process of PDT.

The rate of oxygen consumption may considerably increase in the process of laser irradiation of a tissue in the course of PDT due to the interaction of oxygen with excited PS molecules, which is accompanied by a transition to the singlet state and subsequent oxidation of tissue components. This additional consumption of oxygen may substantially reduce the oxygenation degree of blood in a microcirculatory alveus. Moreover, the capillaries themselves may be also destroyed as a result of PDT. This effect is especially noticeable for photosensitizers using the "vascular mechanism." The predominant destruction of capillaries should be also observed in the case when irradiation with light is performed within a short time interval after the injection of a PS, since a considerable amount of PS still circulates in blood in this case. Thrombosis of capillaries and hemorrhage also lower the mean oxygenation degree of blood. Moreover, this lowering (the vascular effect) is irreversible; i.e., no recovery is observed after the light-irradiation session. This effect can be employed to estimate the efficiency of destruction of a vascular alveus in a tumor in the course of PDT.

KAMIN VIDEO FLUORESCENCE IMAGE ANALYZER (UFF-630/675-01-BIOSPEC)

Uniform irradiation of a biological tissue is one of the main problems encountered in the creation of fluorescence image analyzers. Disadvantages of using a parallel laser beam to irradiate the tissue surface are associated with the fact that the surface of an organ or skin has uneven sections and fragments with a high reflection coefficient, giving rise to shadows and gloss spots. Since some fraction of pump light reaches the

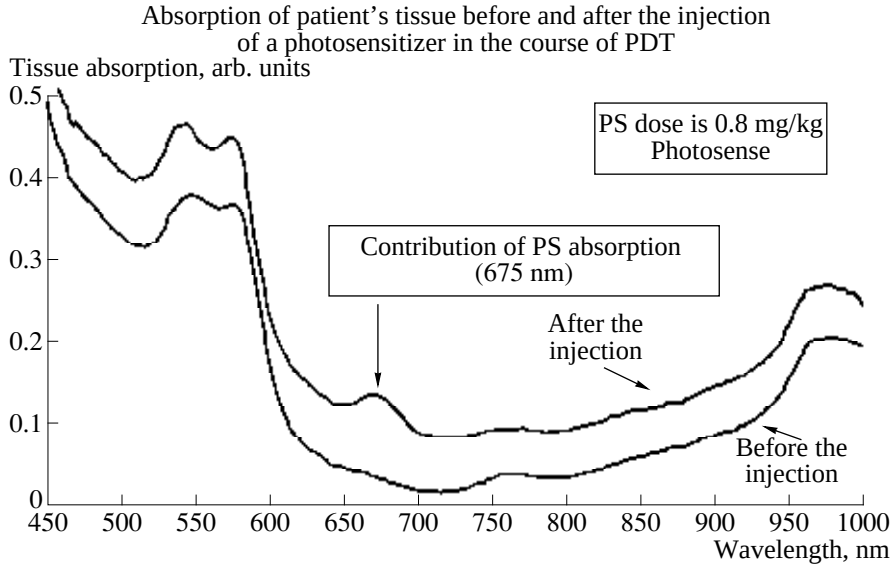

Fig. 8. Absorption spectra of patient's tissue (without corrections for scattering) before and after the injection of 0.8 mg/kg of Photosense photosensitizer. The peak at 675 nm is due to the contribution of the photosensitizer.

detection system, dark and bright sections appear on a fluorescence image. It is usually very difficult to identify these sections properly. To eliminate this difficulty, we developed a conical illumination system with light concentration on the surface of an object. This approach allowed us to get rid of shadows and to considerably suppress gloss spots [Patent 5]. Another serious problem is associated with the speckle structure of laser radiation, which also complicates image processing. To solve this problem, we employed light-emitting diodes with a concentration of light flux as light sources for the analysis of images of surface organs.

We have developed an instrument that can be employed not only for diagnostics, but also for therapy.

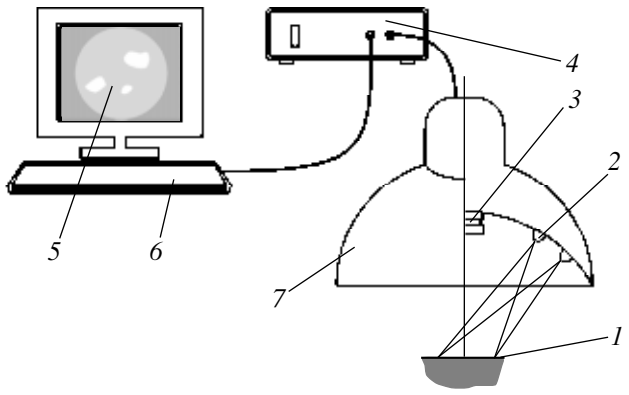

Fig. 9. (*1*) Biological tissue, (*2*) light-emitting diodes, (*3*) CCD camera with a set of filters, (*4*) power-supply and control unit, (*5*) image of a biological tissue, (*6*) personal computer or monitor, (*7*) UFF-630/675-01-BIOSPEC light-emitting-diode video-fluorescence device.

Now, this device is actively used in clinics for intraoperation FD and PDT and for the treatment of various skin diseases (Fig. 9). The developed system includes a high-power light source (1000 mW), which can ensure the energy density of optical radiation up to 40 mW/cm^2. This light source can produce radiation either at 630 or 675 nm and consists of a large number of light-emitting diodes arranged in concentric rings on a spherical surface, ensuring the focusing of light into a spot with a diameter of about 8 cm. A CCD camera and additional light-emitting diodes for IR illumination are located at the center of this surface. When red light irradiates a tissue where a photosensitizer was accumulated, PS excitation gives rise to radiation emission at the fluorescence wavelength. Then, the image is filtered with a set of optical filters and is transmitted by an objective to a CCD camera. The sensitivity of the CCD camera is sufficient (0.05 Lx) for the detection of fluorescent light and the recording of a fluorescence image of a biological tissue. This image may be displayed on a TV screen and recorded on a video. The fluorescence image allows one to locate the areas with the maximum PS concentration, thus revealing the location of a tumor and the areas of possible metastasizing. The created instrument can be also connected to a computer through an appropriate interface, which permits one to digitize and process images. This device can be employed not only for diagnostics, but also for therapy, since the radiation intensity of the light source in this device is sufficient for the excitation of photochemical reactions.

The main advantages of the developed system are associated with its low cost, as the system includes neither expensive laser sources nor complex fiber-optic elements. The use of light-emitting diodes also consid-

erably simplifies the system of electric-power supply and the system of cooling, eventually improving the reliability of the device. Characteristics of the developed device allow one to employ it for photodynamic therapy using the Photosense preparation. The regime of operation with the wavelength of 630 nm is used for preparations based on hematoporphyrin derivatives and 5-ALA (Alasense).

Based on the experience of clinical tests of this device, we have started research and development aimed at creating medical instruments for video-fluorescence diagnostics and PDT of tumors in other localizations, including hollow organs, such as stomach, lungs, bladder, and uterus; abdominal-cavity organs, such as liver, metastasis in peritoneum, ovaries; and skin melanoma.

PDT SYSTEM BASED ON HIGH-POWER LASER DIODES LFT-630/675-01-BIOSPEC

Controlled high-power radiation of a laser system can be employed for a photodynamic therapy of abdominal-cavity, intratissue, and surface tumors. This system is equipped with a set of fiber-optic catheters for different localizations, including lungs, stomach, bladder, mammary gland, etc. The radiation wavelength employed in the LFT-675-01-BIOSPEC system is optimal for PDT with the use of the Photosense preparation (Research Institute of Organic Polymers and Dyes). The LFT-630-01-BIOSPEC laser system is employed for therapy with photosensitizers based on hematoporphyrin derivatives and 5-ALA. The maximum radiation power achieved at the output of the optical unit of the laser system is 2 W (a power of up to 1.2 W can be achieved at the output of the fiber-optic catheter). The system allows the radiation power to be controlled and the required irradiation time to be set. The irradiation dose is calculated automatically. The system is based on a laser diode with a high reliability [Patent 6] and a large service lifetime. The created laser system is very compact. It requires neither special maintenance nor water cooling and is ready for operation right upon the turn-on. The laser system can be also assembled in a DIN41494 standard and mounted on a 19″ bench.

PROPAGATION OF LASER RADIATION IN A BIOLOGICAL TISSUE UNDER CONDITIONS OF PHOTODYNAMIC THERAPY AND DIAGNOSTICS

We have investigated the propagation of visible laser radiation (675 nm) in biological tissues. The purpose of these studies was to accumulate experimental data for subsequent modeling of tissues whose parameters correspond to a tumor. Such a reference tissue is necessary for the development of practical instructions on photodynamic therapy. We have studied fatty and muscular tissues of animals. The data on optical properties of living tissues (ear lobe, palm, and tip of an index finger) are also available from [21].

The idea of the first experiment can be described in the following way. We measure the distribution of the power density in the air gap between the catheter and the photodetector. Then, a fatty or muscular tissue layer with a thickness of 2, 4, and 6 mm is placed in front of the power meter, and the measurements are repeated. A diagram of the experimental setup is shown in Fig. 10. An optical catheter is fixed to a vertical holder. Measurements are performed with a step of 2 mm. We measured the power density of laser radiation transmitted through a tissue layer and the diameter of the laser spot on the surface of a sample. A diode laser with an output power of 2 W and a wavelength of 675 nm was used as a source of radiation. The results of measurements performed for a fatty tissue are presented in Fig. 10.

The next experiment was performed in the following way. A parallelepiped was cut out of a muscular or fatty biotissue. An optical catheter with a cylindrical diffuser was placed inside this sample in such a way that the distance between the catheter and the sample walls was 5, 10, 15, and 20 mm. A photodetector was placed on the face of the parallelepiped. Measurements were performed with the same laser generating radiation with a power of 500 mW. The results of these measurements are presented in Fig. 11.

In the third experiment, an end optical catheter was placed inside a layer of a muscular or fatty biological tissue at different distances from the photodetector. Dependences measured in these experiments are shown in Fig. 12.

In the process of PDT, one often encounters the problem of achieving a high power density of laser radiation in tissue layers located far (5–15 mm) from the tissue surface. Since absorption and scattering make laser radiation weaker as the distance from the surface of a medium increases, the surface power density of laser radiation may considerably exceed the level acceptable for laser therapy.

Therefore, the possibility of estimating the distribution of radiation energy density for different types of tissues and irradiation geometries is the necessary condition for successful PDT. An idea of focusing radiation inside a tissue is also very attractive. Such a focusing would increase radiation concentration and either partially or completely compensate for light attenuation due to scattering and absorption.

In the case of laser-fluorescence diagnostics of biological tissues with the use of optical fibers, it is important to know which volume of tissue serves as a source of the measured light flux and how this volume (the volume of probing) is positioned with respect to optical fibers delivering and collecting light.

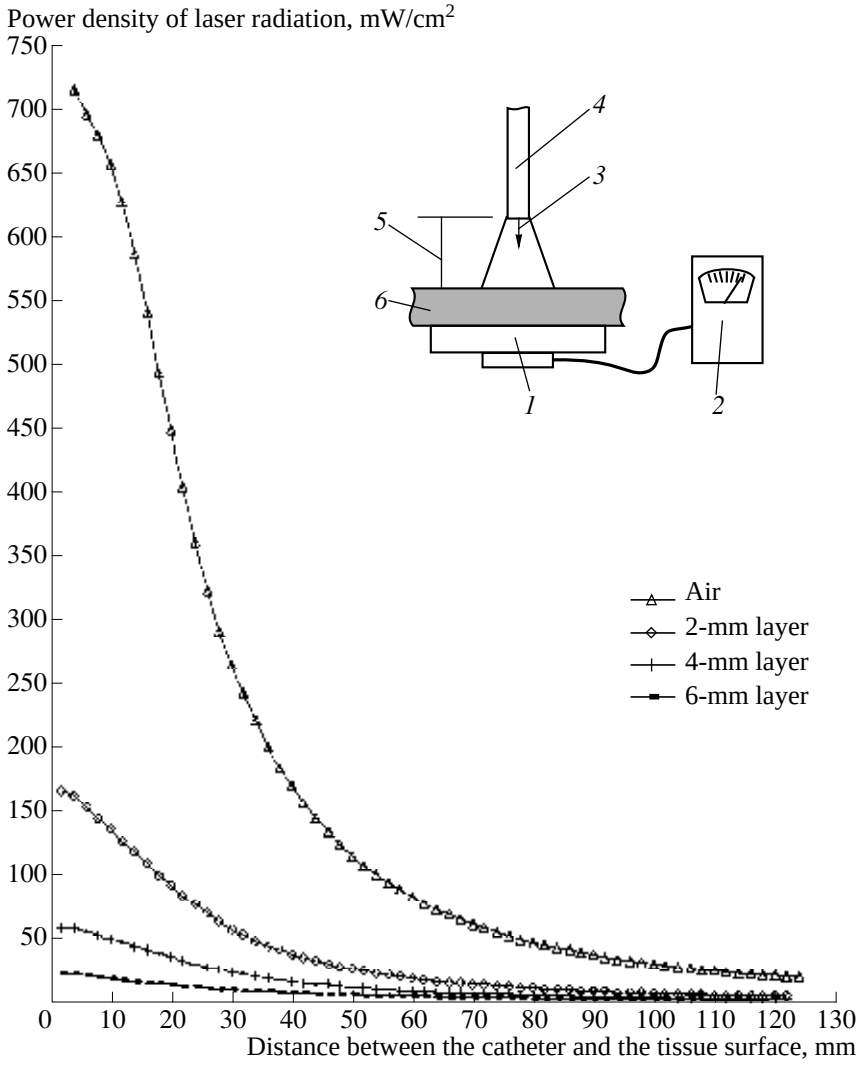

Fig. 10. The power density of laser radiation transmitted through a tissue layer as a function of the distance between an optical catheter and the tissue surface. A fatty tissue. (*1*) Photodetector, (*2*) indicator, (*3*) optical radiation, (*4*) fiber-optic catheter, (*5*) distance between the fiber-optic catheter and the detector, and (*6*) biological tissue.

In cases of practical importance when a single fiber brought in contact with a tissue is used to irradiate the tissue and to collect radiation backward-scattered by this tissue or when the transmitting and receiving fibers are located adjacent to each other, it is most likely that the volume of measurements is localized around the fiber ends. Such a situation arises in the case of an optically uniform medium. However, most of biological tissues are optically nonuniform, and the latter statement may become invalid in this case. Such an arrangement of receiving and transmitting fibers is widely used for endoscopic studies in clinical practice.

The volume and the shape of the area of measurements in such a geometry depend on optical characteristics of a medium: the absorption coefficient μ_a; the scattering coefficient μ_s; the phase function $P(\theta)$, which characterizes the radiation pattern of a single scatterer; and the geometry and optical characteristics of optical fibers.

The propagation of optical radiation through a scattering medium is usually analyzed with the use of the Monte Carlo method [14, 15], when random-walk trajectories of a large number of photons in a scattering medium from the transmitting fiber to the receiving fiber are simulated. Then, the spatial areas enclosing most of these trajectories are determined. These areas have a characteristic banana shape. Monte Carlo simulations are labor and time consuming. In addition, this approach does not allow one to include effects of multiple scattering and cannot be applied within the entire range of parameters of scattering optical media.

In this paper, we employ the theory that was used by Kiselev, Lin'kov, and Loschenov in 1996 to calculate

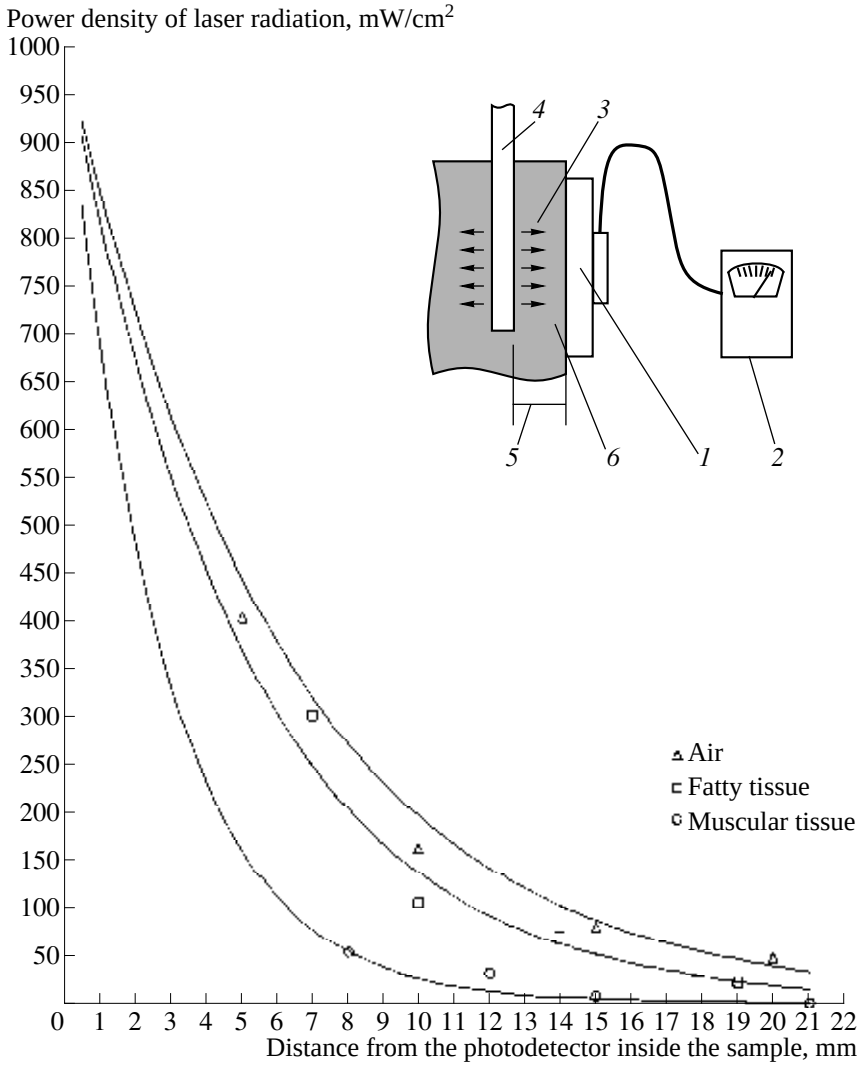

Fig. 11. Distribution of the power density of laser radiation inside a sample of biological tissue. (*1*) Photodetector, (*2*) indicator, (*3*) optical radiation, (*4*) fiber-optic catheter, (*5*) distance between the fiber-optic catheter and the detector, and (*6*) biological tissue.

the distribution of optical radiation in a scattering biological medium [22, 23]. A biological medium within the framework of this approach is modeled as a three-dimensional structure of optically connected areas with unique optical properties. This model includes effects of multiple scattering of light not only for adjacent areas, but for all the areas in the medium.

THEORY

A biological medium is discretized with the use of areas V with attached waveguide channels. Forward waves (the waves from pump sources) reach a volume V through waveguide channels. Scattering in all the channels gives rise to backward waves, which produce a diffraction response of the area V to radiation coming from the outside. The linearity of Maxwell equations governing linear media permits us to consider a backward, or an output, wave B_i as a sum of forward, or input, waves A_j multiplied by some constant coefficients S_{ij}.

Thus, the scattering process considered as a response of a medium to pump radiation is characterized by the relation

$$\begin{bmatrix} B_1 \\ B_2 \\ \dots \\ B_N \end{bmatrix} = \begin{bmatrix} S_{11} & S_{12} & \dots & S_{1N} \\ S_{21} & S_{22} & \dots & S_{2N} \\ \dots & \dots & \dots & \dots \\ S_{N1} & S_{N2} & \dots & S_{NN} \end{bmatrix} \begin{bmatrix} A_1 \\ A_2 \\ \dots \\ A_N \end{bmatrix} \quad (1)$$

which can be written in the reduced form $[B] = [S]*[A]$, where $[A]$ is the column matrix $(N \times 1)$ characterizing input, or incident, waves; $[B]$ is the column matrix $(N \times 1)$ characterizing output, or reflected, waves; $[S]$ is the square matrix $(N \times N)$ representing the scattering matrix; and N is the number of waveguide channels connecting the area V.

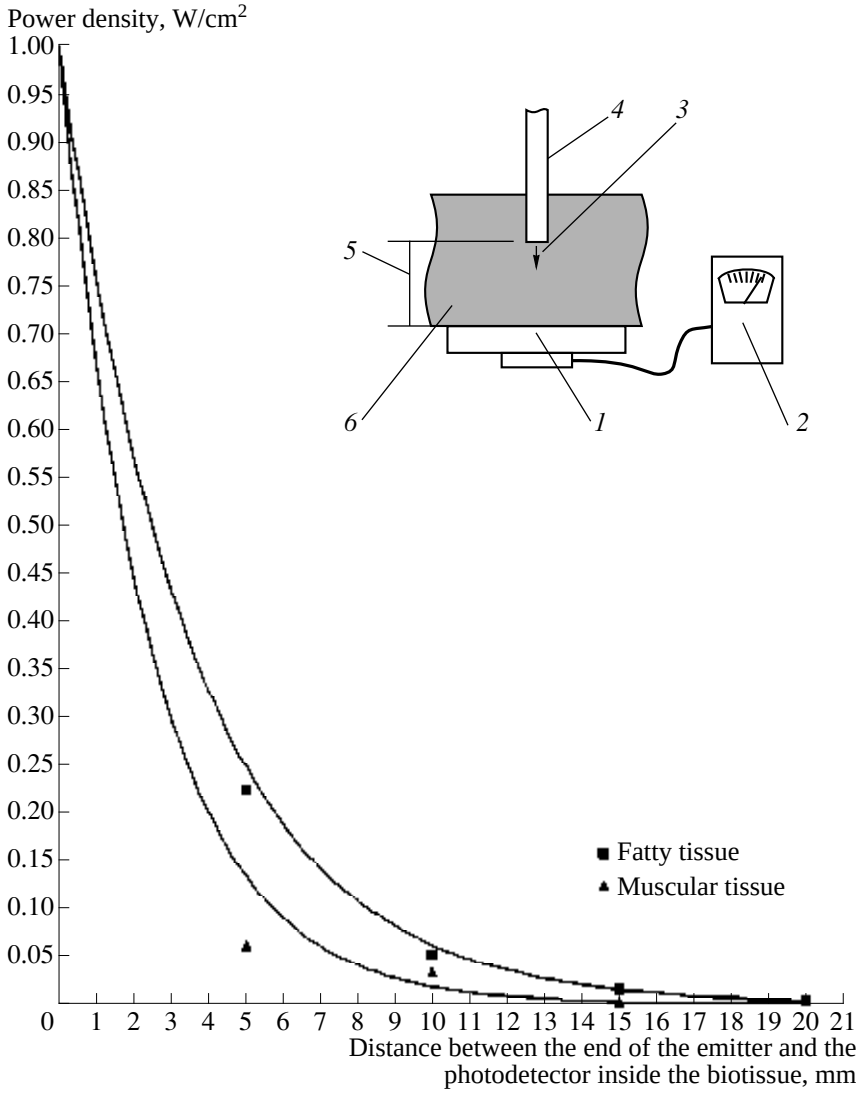

Fig. 12. Distribution of the power density of radiation inside a biological tissue (end emitter, transmission geometry). (*1*) Photodetector, (*2*) indicator, (*3*) optical radiation, (*4*) fiber-optic catheter, (*5*) distance between the fiber-optic catheter and the detector, and (*6*) biological tissue.

We can also write

$$[B] = [S]*[A] + [Q]*[C], \tag{2}$$

where $[Q]$ is the radiation matrix and $[C]$ is the field of internal radiation sources.

To calculate the distribution of the scattered fraction of radiation over waveguide channels, we have to employ an additional information on the radiation pattern of a single scatterer. The Henyey–Greenstein function corresponds to an elementary one-parameter model of a single scatterer:

$$p(\theta) = \frac{(1-g)^2}{(1+g^2-2\cos\theta)^{\frac{3}{2}}}, \tag{3}$$

where g is the only parameter characterizing the anisotropy of scattering and θ is the angle measured from the initial direction of radiation (the scattering angle).

If the elementary area is connected with the neighboring areas by means of N waveguide channels, then the probability of scattering into the Jth waveguide channel is equal to

$$p(\theta) = \frac{\int_{\theta_J}^{\theta_{J+1}} p(\theta)d\theta}{\int_0^{2\pi} p(\theta)d\theta}. \tag{4}$$

Due to the symmetry of the phase function for N symmetric waveguide channels, the phase function may take $N/2 + 1$ different values. The elements of the scattering matrix for an elementary area ΔL can be written as

$$S_1 = \exp(-\mu_a \Delta L)[p(\theta_1) + \exp(\mu_s \Delta L)(1 - p(\theta_1))],$$
$$S_j = \exp(-\mu_a \Delta L)(1 - \exp(-\mu_s \Delta L) p(\theta_j)). \quad (5)$$

Determining the scattering matrix for a medium as a whole by joining optically connected areas, we can find both internal and external fields for arbitrarily chosen fields of pump radiation sources, an arbitrary geometric structure of the scattering medium, and unique optical parameters of each subelement of an optically nonuniform medium.

Algorithm of Simulations

For simplicity, we consider a two-dimensional model of a biological medium. An algorithm of simulations implies that the distribution of the field $F(x, z)$ is calculated in the xz-plane (where x is the transverse coordinate and z is the depth) in the case when the radiation source (the end of the fiber transmitting laser radiation) is located at the point with coordinates $(X_{1,0})$ on the surface of the medium. The set of initial data for simulations included the waveguide geometry, the angular orientation of the optical fiber with respect to the surface of the medium, and the geometry and optical parameters of a biological medium (coefficients of absorption and scattering and the G factor). Then, we calculated the distribution of the fluorescence field for a spatially distributed fluorescence source located inside the medium. The local intensity of the light flux from this source is proportional to the absorbed fraction of laser radiation.

The next stage of simulations implied the calculation of the spatial distribution of the field $Q(x, z)$ that can reach a photodetector (the end of the receiving fiber) positioned at the point with coordinates (X_2, Z_{max}) on the surface of the medium in the case when transmitted radiation is detected and at the point with coordinates $(X_2, 0)$ if reflected radiation is detected in the case when the rear side of the medium is not accessible.

Finally, we calculate the contributions of different areas V of the medium to the signal registered by a photodetector:

$$V(x, z) = 1 - F(x, z)\frac{Q(x, z)}{M}, \quad (6)$$

where M is the normalizing factor, which is chosen in such a way that $\iint V(x, z)dxdz = 1$ for the entire volume of the scattering medium.

Let us consider several specific examples of using this algorithm for calculating the energy density for a medium with optical parameters characteristic of certain biological tissues. Virtually all the soft biological tissues and blood have an optical anisotropy equal to 0.8–0.95. Parameters of skin vary from sample to sample within a broad range due to the horny epidermis layer. The optical anisotropy of skin can be taken equal to 0.5, although this approximation is rather rough.

Figure 13 presents the distribution of scattered laser radiation (633 nm) and fluorescence (680 nm) with allowance for optical coefficients and the anisotropy factor characteristic of human skin without epidermis. As can be seen from these data, energy density is mainly concentrated within a layer whose depth does not exceed 2 mm. The distribution of fluorescence is much deeper, reaching 5 mm.

Figure 14 displays the distribution of scattered laser radiation and fluorescence for a tissue irradiated with a broad beam. As can be seen from this figure, the relation between scattered radiation and fluorescence remains unchanged.

Figure 15 shows a diagram representing the distribution of energy density involved in signal formation in diagnostic studies of biological tissues with the use of a diagnostic catheter. The probed volume with such a fiber geometry is 2 mm^3.

Diagrams in Fig. 16 represent the distribution of energy density in a biological medium with an anisotropy factor $G = 0.85$ in the case when radiation (675 nm) is focused at a depth of 5 mm. As can be seen from this diagrams, the focusing of radiation leads to energy concentration at a depth of 5 mm. However, when performing a photodynamic therapy of a tumor, one has to take into account the fact that, if radiation passes through the epidermal layer, the diagram changes.

Figure 17 displays a diagram representing the distribution of energy density of radiation in the case when laser light is delivered by two optical fibers located at a distance of 15 mm from each other. An identical diagram is observed when one fiber emits radiation, while the other one receives the light. Only in this case, the area of maximum density determines the area of probing. Numbers in the diagram indicate the relative values of energy density normalized to unity. In other words, the isoenergy surface, whose contour is shown at the center, contains 20% of the entire energy density. The diagrams are arranged in a sequence from $G = 0$ to $G = 0.9$ with a step of 0.1. As can be seen from these diagrams, the probed volume considerably depends on the G factor. With $G = 0$–0.5, the information is extracted from the depth of 2–3 mm. For $G = 0.5$–0.9, the studied signal comes from the near-surface area where the receiving fiber is brought in contact with a biological tissue.

Recently, our group in collaboration with G.L. Kiselev developed a computer code allowing real-time simulation of diagrams representing energy density distributions for different optical properties of tissues, various photosensitizers, and different radiation

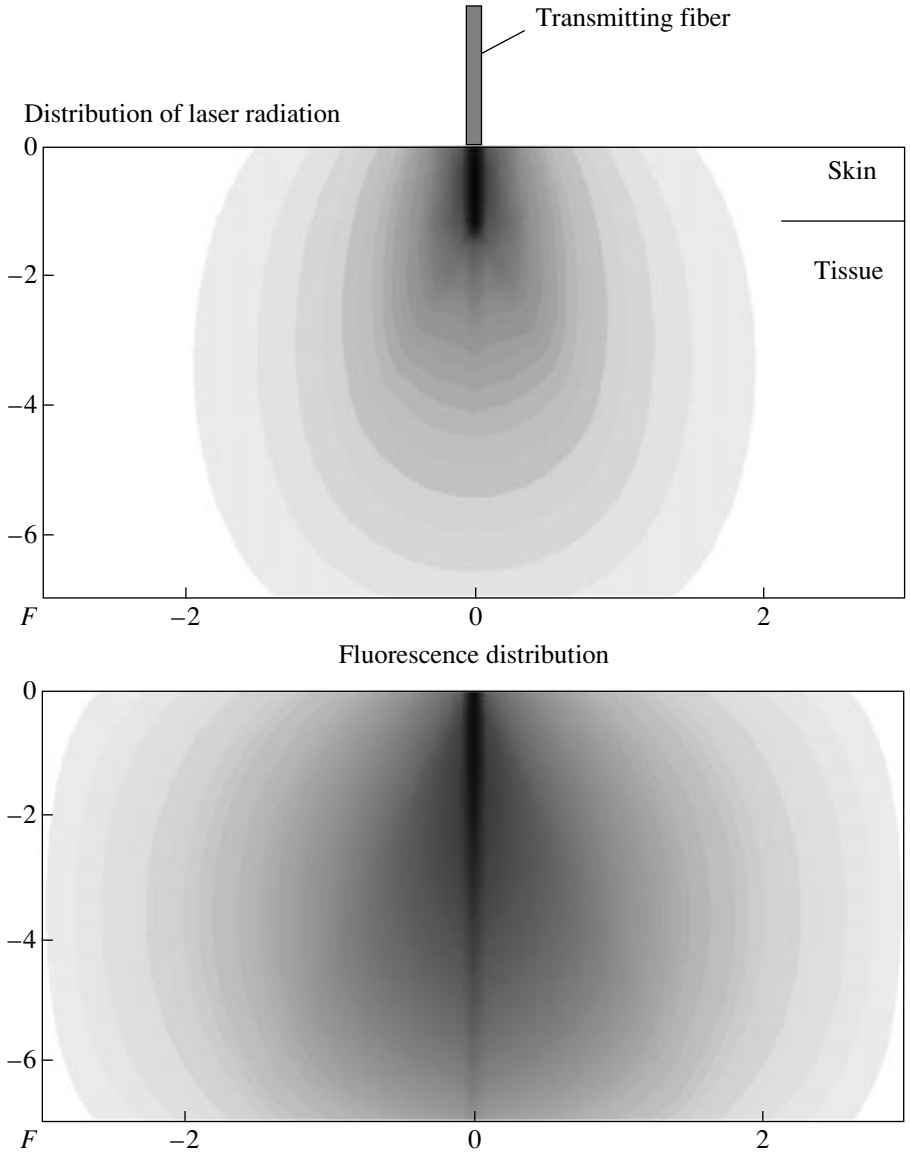

Fig. 13. Distribution of scattered laser radiation and fluorescence for a biological tissue irradiated with a thin beam.

wavelengths and characteristics of optical fibers delivering radiation to a biological tissue.

Our theoretical calculations demonstrate the possibility of using optical methods not only for a diagnostics, but also for a therapy of tumors located far from the surface with a minimal damage for healthy tissue areas.

EXPERIMENTAL ASSESSMENT OF THE EFFICIENCY OF PHOTOSENSITIZERS

No more than ten different photosensitizers are currently employed in clinical practice throughout the world. About 50 photosensitizers are in the phase of experimental investigations. There is also a large number of preparations that can be, in principle, used for FD and PDT. The potential efficiency of photosensitizers is determined by several factors, including

—a low dark toxicity of doses employed in practice;

—a high rate of PS removal from organism;

—selective capture of a photosensitizer by tumor cells and tissues;

—a high quantum yield of generation of singlet oxygen;

—radiation wavelength should fall within the transparency window of a biological tissue or should be close to this window;

—reasonable cost of the preparation.

Interaction between a photosensitizer, photons of light, and oxygen molecules leads to the production of active forms of oxygen, such as singlet oxygen, oxygen

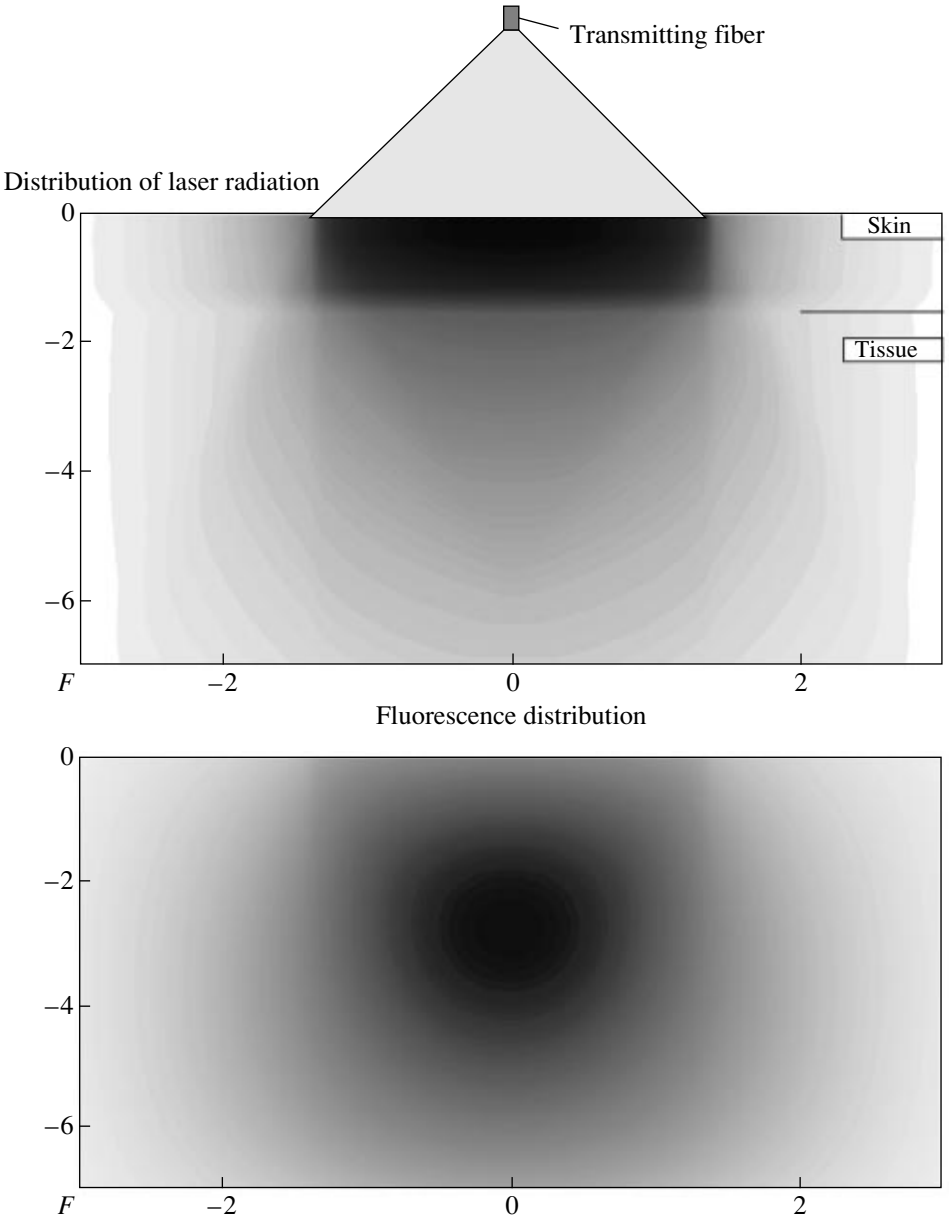

Fig. 14. Distribution of energy density in a biological tissue irradiated with a broad beam.

radicals, etc. These forms of oxygen may destroy proteins in inter- and intracellular liquid, as well as proteins entering into cellular membranes. In accordance with these concepts, the level of oxygen consumption (the decrease in oxygen concentration per unit time) in the course of PDT should correspond to the level of active photodynamic processes, such as the destruction of proteins, intracellular structures, and cellular membranes. This may imply that the efficiency of a photodynamic reaction can be estimated from the level of oxygen consumption within the irradiated volume of a biological tissue.

Since the correlation between the concentration of dissolved oxygen in blood and hemoglobin oxygenation (O_2-sat) inside erythrocytes is strong, photodynamic reactions in whole blood can be monitored by measuring the O_2-sat level (%).

Another important aspect of studying a photodynamic process is associated with the determination of the PS concentration in an irradiated tissue. Reversible and irreversible photobleaching effects may give rise to a clearly pronounced change in the photodynamic dose in the course of PDT. Studying the dynamics of photobleaching in blood, one can reveal real changes in the PS concentration in a biological tissue.

The table presents the results of studies performed by our group in collaboration with A.Yu. Duplik

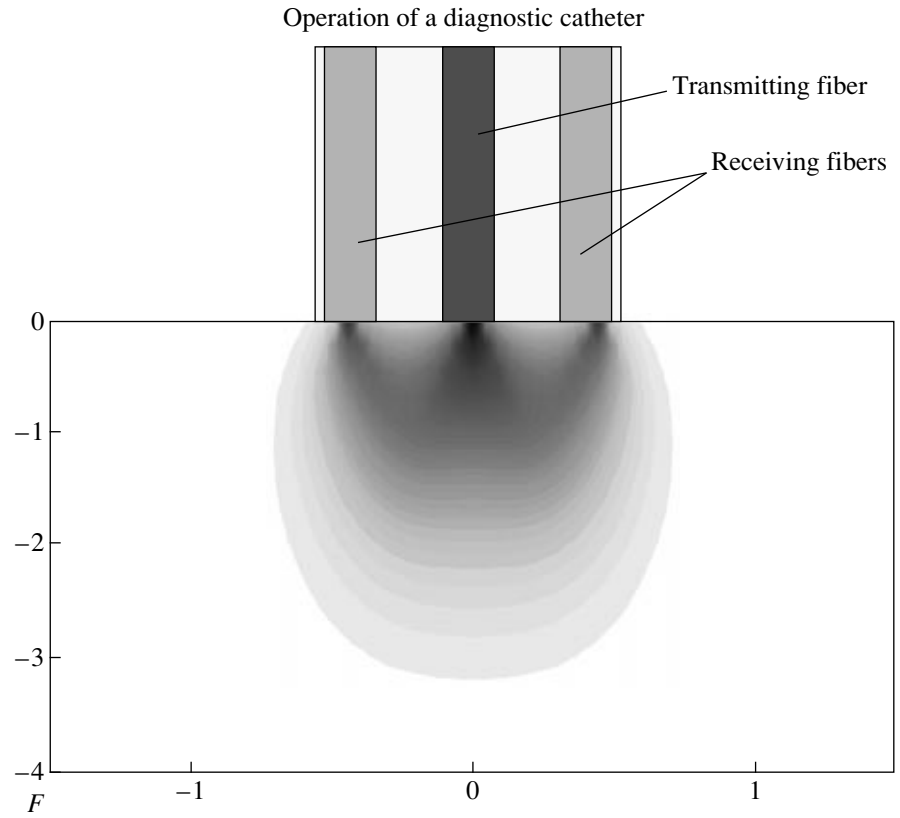

Fig. 15. Diagram of energy distribution in the case of a diagnostic catheter.

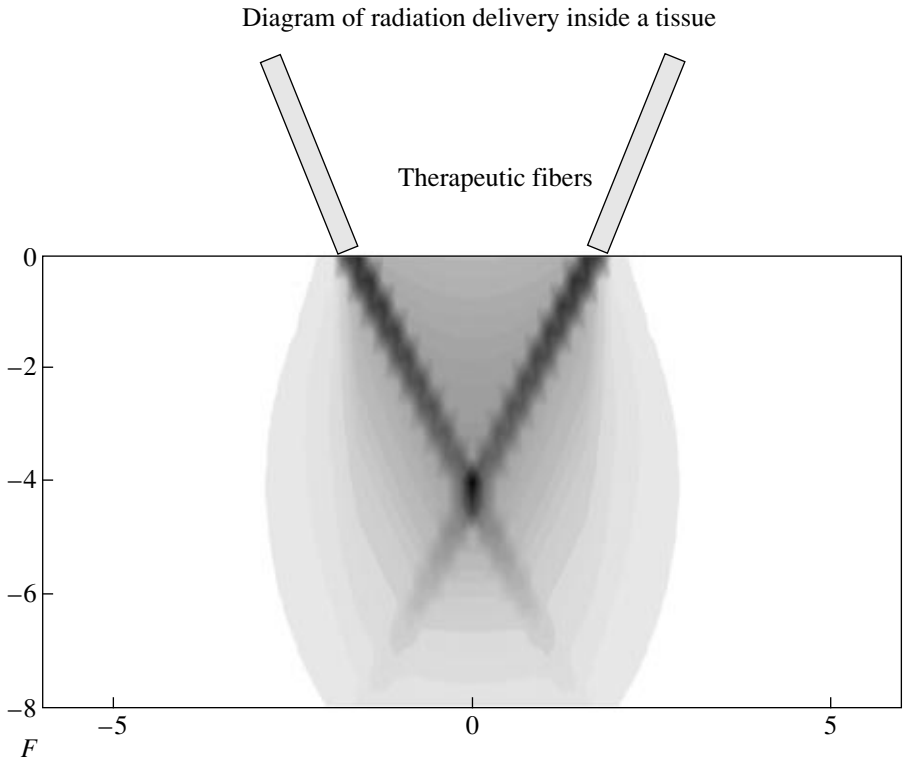

Fig. 16. Diagrams of energy density distribution in a biological tissue with $G = 0.85$. Radiation is focused at a depth of 5 mm inside the tissue.

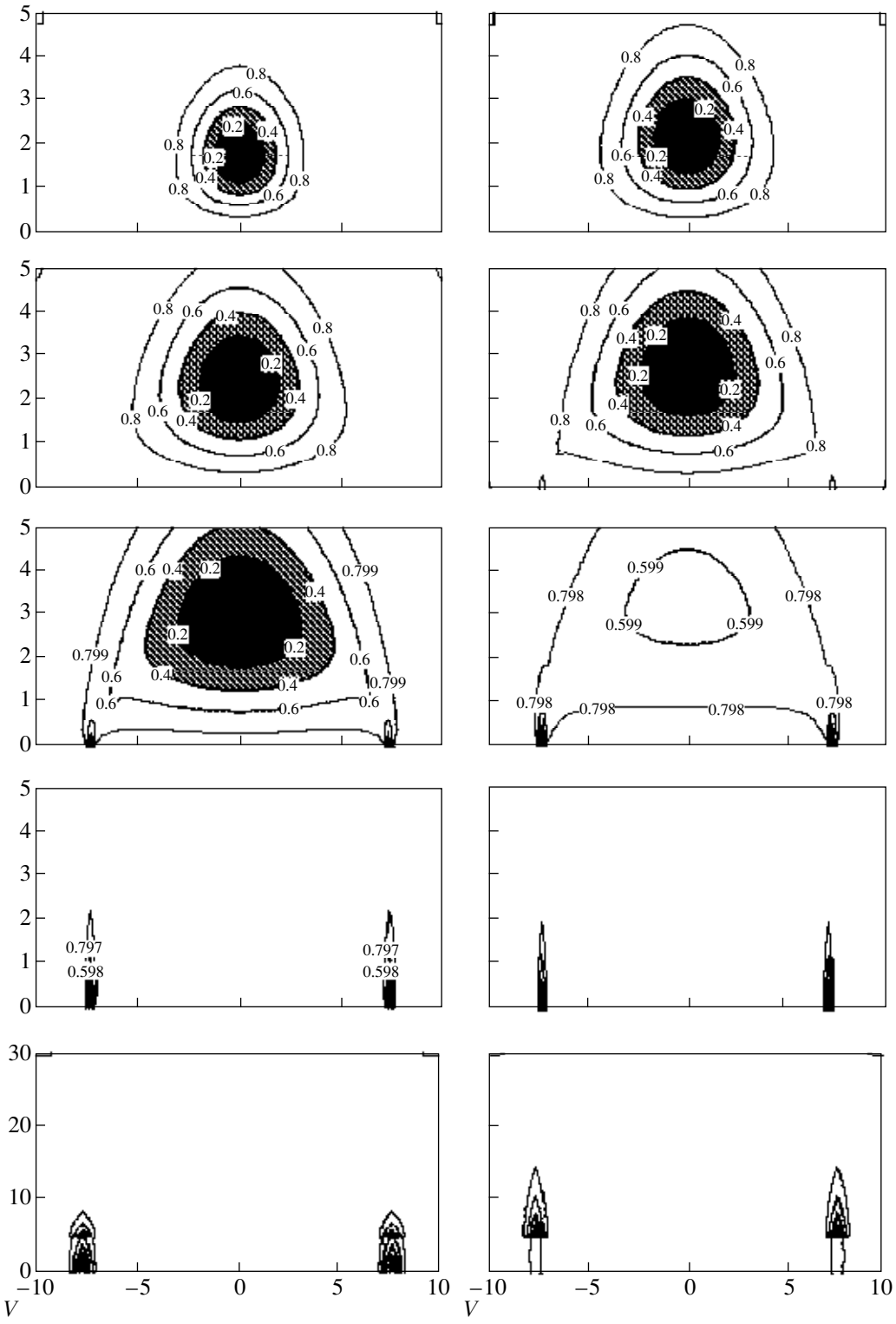

Fig. 17. Isoenergy curves for scattered laser radiation in a biological tissue with different *G* factors. The distance between the optical fibers is 15 mm.

[24, 25] on some of the photosensitizers that are of practical interest for PDT.

Parameters of fluorescence and photobleaching and its reversibility were measured for samples of whole blood, whole-blood components, and a PS solution with the use of a LESA-6 fiber-optic spectrofluorometer. These measurements were performed in a cell [Patent 7] for a 1-mm-thick layer of liquid placed in a

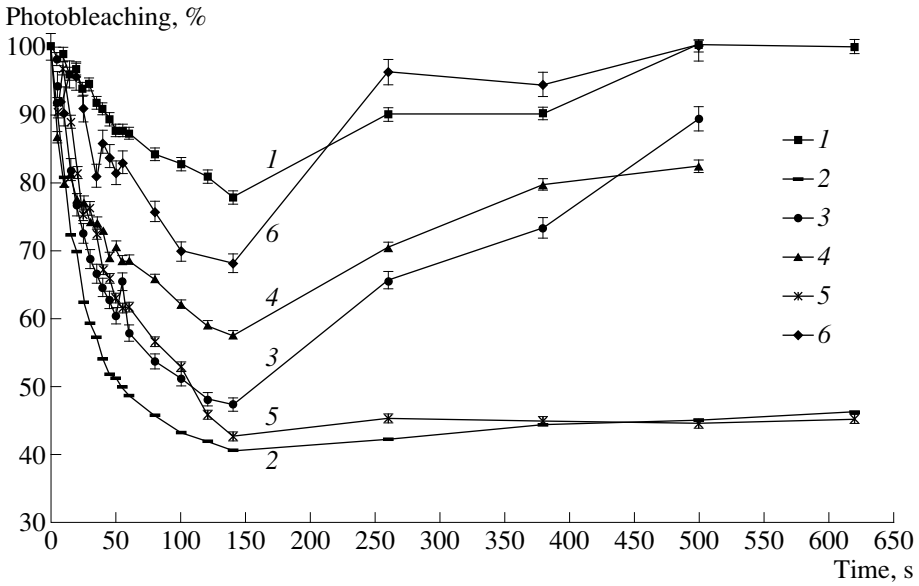

Fig. 18. Photobleaching of the studied photosensitizers in precipitated erythrocytes. The photobleaching is measured as a percentage of the photobleaching in a test sample (parameters of a sample within the first few seconds after the excitation): (*1*) chlorine p6 I, 0.01 mg/ml; (*2*) chlorine p6 II, 0.01 mg/ml; (*3*) hematoporphyrin (Photogem), 0.05 mg/ml; (*4*) aluminum phthalocyanine (Photosense), 0.001 mg/ml; (*5*) zinc phthalocyanine IV, 0.013 mg/ml; and (*6*) methylene blue, 0.01 mg/ml. No photobleaching of studied photosensitizers was observed for a PBS solution and blood plasma.

special light-proof holder. We left blood in the cell for 2 h for the separation of blood into plasma and erythrocytes. Fluorescence was excited with a He–Ne laser.

The photobleaching was monitored from the change in the ratio of the area of the spectrum of the pump source to the area of the fluorescence spectrum.

The dynamics of the process of photodynamic deoxygenation *in vitro* is presented in Fig. 18.

Comparing deoxygenation curves, we find that the highest rate of photodynamic deoxygenation is achieved when whole blood is photosensitized with zinc phthalocyanine IV. We were not able to detect the deoxygenation of uroporphyrin III even when P_v was increased up to 0.3 W/cm^2 (λ = 675 nm). No clearly pronounced deoxygenation was also observed for hematoporphyrin (Photogem) irradiated by light with λ = 633 nm and P_v = 0.1 W/cm^2.

Figures 19a–19c present the results of fluorescence measurements performed for the studied photosensitizers in the solution of a PBS buffer in whole blood and its components.

The results of these spectral measurements demonstrate that, when a photosensitizer is dissolved in blood and becomes related to blood components, including plasma proteins or erythrocytes, the shape of the spectrum changes and the maximum of fluorescence is shifted relative to the maximum of fluorescence observed for the solution of this photosensitizer in a PBS buffer.

Figure 20 displays the results of photobleaching monitoring. We observed no photobleaching for the studied photosensitizers in a PBS solution and blood plasma.

Comparative analysis of the measured dependences has shown that zinc phthalocyanine IV is a photosensitizer that ensures a maximum rate of blood photodynamic deoxygenation. This photosensitizer is a mixture of approximately equal amounts of tetrasulfonated (46%) and trisulfonated (44%) compounds with an addition of disulfonated compounds (10%).

We have also revealed a photosensitizer ensuring the maximum rate of photobleaching in whole blood and precipitated erythrocytes. We should note that the maximum fluorescence intensity decreases, on the average, by a factor of 5–6 within 4–6 min during the photobleaching process.

Methylene blue features an absolutely reversible photobleaching in precipitated erythrocytes and displays the highest photobleaching inversion rate among the studied photosensitizers. The initial fluorescence spectrum of methylene blue is recovered within 6 min.

In cooperation with S.S. Kharnas and A.A. Stratonnikov, we have developed an original technique for estimating the efficiency of a photosensitizer from the generation of singlet oxygen in cell cultures. This method can be described in the following way. Blood erythrocytes and a photosensitizer being tested are added to a cell culture, which is irradiated with light whose wavelength corresponds to the red edge of the PS absorption spectrum. Then, the spectrum of backward scattering is

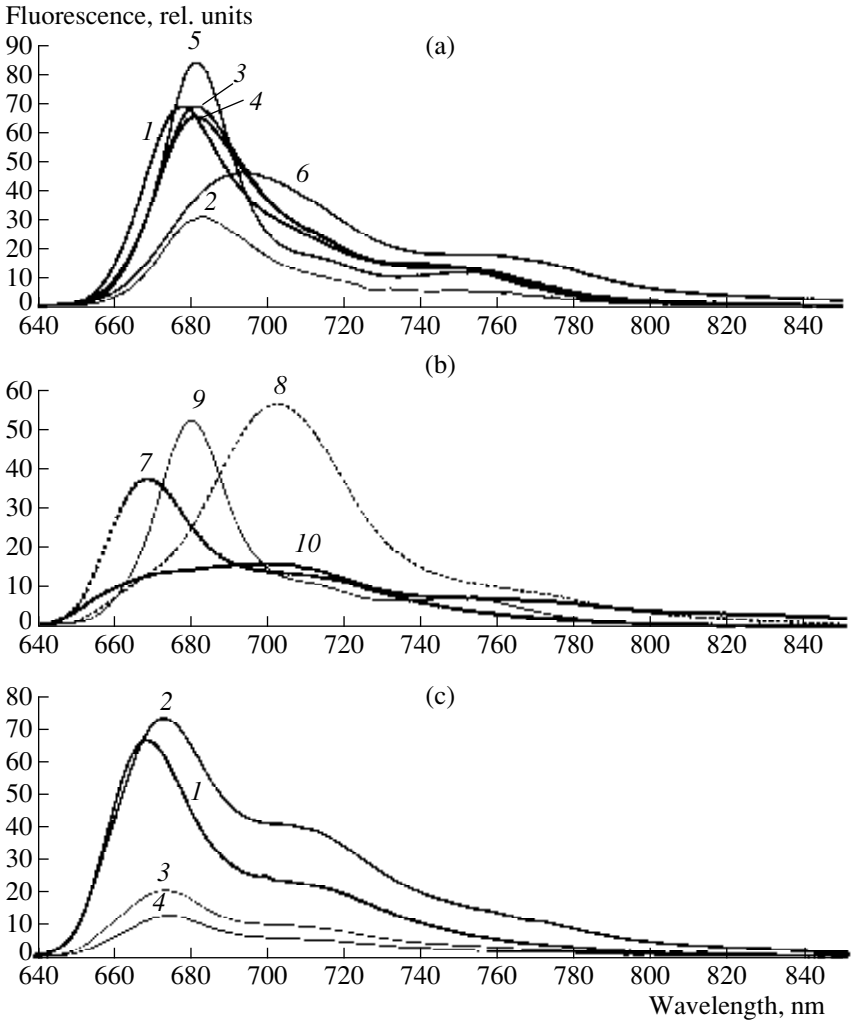

Fig. 19. (a) Fluorescence spectra of the studied photosensitizers in a PBS buffer: (*1*) aluminum phthalocyanine (Photosense), 0.01 mg/ml; (*2*) zinc phthalocyanine I, 0.0135 mg/ml; (*3*) zinc phthalocyanine II, 0.0128 mg/ml; (*4*) zinc phthalocyanine III, 0.0119 mg/ml; zinc phthalocyanine IV, 0.013 mg/ml; (*5*) chlorine p6 I, 0.01 mg/ml; (*6*) chlorine p6 II, 0.01 mg/ml; (*7*) methylene blue, 0.01 mg/ml; and (*8*) hematoporphyrin (Photogem), 0.03 mg/ml; uroporphyrin III, 0.023 mg/ml. (b) Fluorescence spectra of methylene blue (0.01 mg/ml) in (*1*) a PBS buffer, (*2*) whole blood, (*3*) plasma, and (*4*) erythrocytes. (c) Fluorescence spectra of hematoporphyrin (Photogem) (0.03 mg/ml) in (*1*) a PBS buffer, (*2*) whole blood, (*3*) plasma, and (*4*) erythrocytes. As can be seen from the presented spectra, when a photosensitizer is dissolved in blood and becomes related to blood components (plasma proteins or erythrocytes), the shape of the spectrum changes and the maximum of fluorescence is shifted with respect to the maximum of fluorescence from the solution of the considered photosensitizer in a PBS buffer.

employed to determine the dynamics of changes in the oxygenation degree of hemoglobin in erythrocytes. Using this approach, we can estimate the amount of singlet oxygen produced by a single PS molecule per unit absorbed power. Living and dead cells have been simultaneously calculated, and the character of cell death was assessed (necrosis, apoptosis, and oncosis). Sulfonated aluminum phthalocyanine and sulfonated zinc phthalocyanine displayed the highest activity among 20 studied photosensitizers. Similar studies were also performed on experimental animals with grafted tumors. These experiments confirmed the results obtained earlier in studies with tissue cultures.

THE USE OF FD AND PDT METHODS IN CLINICAL PRACTICE

The methods of FD and PDT were employed for a diagnosis and treatment of tumors in more than 2000 patients at I.M. Sechenov Moscow Medical Academy and N.N. Blokhin Oncological Research Center, Russian Academy of Medical Sciences. The best results were achieved for stomach cancer, lung cancer, head and neck tumors, and bladder cancer. Photodynamic therapy gave the best results in the cases of stomach cancer, lung cancer, skin cancer, and head and neck tumors [26–35]. Methods for a diagnosis and treatment of gynecological diseases, urological dis-

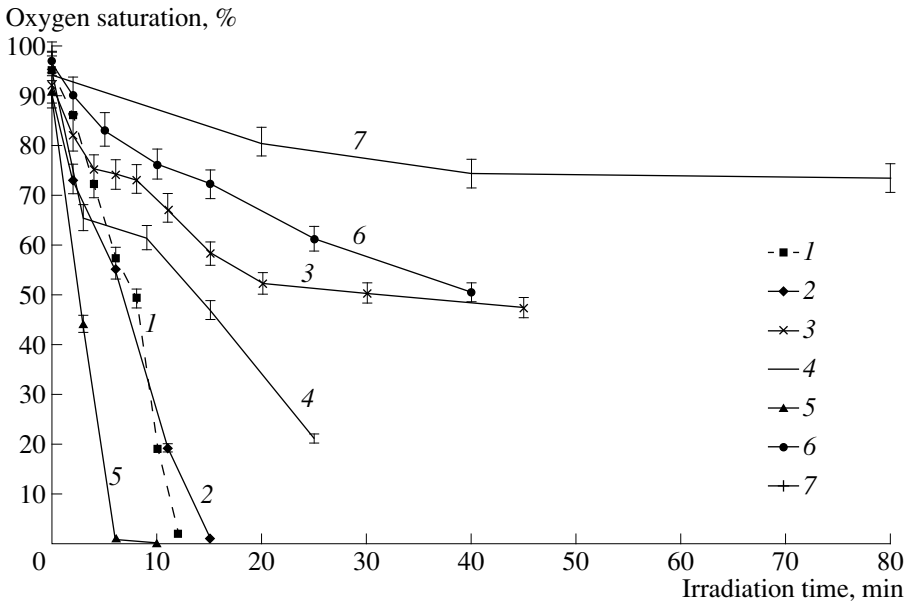

Fig. 20. Monitoring of photodynamic deoxygenation *in vitro* on whole blood by the method of a glass sandwich. Samples are irradiated with a light with λ = 665–675 nm and P_V = 0.010 W/cm^2: (*1*) aluminum phthalocyanine (Photosense), 0.01 mg/ml; (*2*) zinc phthalocyanine I, 0.0135 mg/ml; (*3*) zinc phthalocyanine II, 0.0128 mg/ml; (*4*) zinc phthalocyanine III, 0.0119 mg/ml; zinc phthalocyanine IV, 0.013 mg/ml; (*5*) chlorine p6 I, 0.01 mg/ml; and (*6*) chlorine p6 II, 0.01 mg/ml. Measurements carried out with the use of a MicroAstruba analyzer revealed the lowering of pO_2 in irradiated samples from 100–170 mm Hg down to 0–2 mm Hg, with pH and pCO_2 remaining virtually unchanged. An attempt of repeated oxygenation of the irradiated blood sample was successful. The oxygenation level was recovered, in accordance with the results of gas analysis, up to about 97%.

eases, and benign tumors with different localizations, as well as infectious diseases, including tuberculosis, are being developed now.

The goal of physicists is not to restrict themselves to technical studies, but also to develop the methods of irradiation and techniques for testing the treatment process [Patents 8–12]. Several examples are given below.

—When a tumor is irradiated with laser light, a photosensitizer inside this tumor is bleached and loses its activity. In addition, the thrombosis of vessels limits the access to the irradiated volume for oxygen. Consequently, efficient PDT is possible only when these parameters are monitored in such a way that the tactics of irradiation can be timely changed.

—We have found that, if a tumor is irradiated with a low-power light before the introduction of a photosensitizer, then the PS concentration considerably increases with the same dose of introduction, which allows the dose of introduced PS to be reduced and, correspondingly, the toxicity and the costs of treatment to be lowered [Patent 1].

—Irradiation of liver metastases with ultrasonic control requires a special modeling for the determination of irradiation parameters as functions of the PS concentration inside a metastasis area and on its boundary. In this case, we had to solve the problem of how to irradiate the entire tumor volume uniformly having a needle catheter in our tool kit.

—The therapy of hollow organs, such as a bladder and uterus, requires high-precision systems of laser-radiation delivery to disease tissue areas, which are often invisible for a naked eye. This problem is being solved at the moment.

—Skin melanoma is one of the tumors that are especially difficult to cure. Tumors of this kind are dangerous because, being treated from the outside, they start to rapidly metastasize, giving rise to metastases inside the skin, which are difficult to detect. Therefore, we are working now on the detection of intraskin metastases using special approaches allowing the sensing of changes in optical parameters of skin from the surface to deeper layers. The PDT problem can be solved by focusing laser radiation and irradiating a tumor, gradually scanning the beam from deeper layers to surface layers.

ACKNOWLEDGMENTS

We are grateful to the personnel of the Laboratory of Laser Biospectroscopy, whose results are presented in this review. We are also thankful to the personnel of I.M. Sechenov Moscow Medical Academy; N.N. Blokhin Oncological Research Center, Russian Academy of Medical Sciences; and NIPIK State Research Center of Russian Federation for their active help and cooperation in this research.

REFERENCES

1. Chissov, V.I., Sokolov, V.V., and Filonenko, E.V., 1998, *Ross. Khim. Zh.*, **XLII**, no. 5, 5.
2. Luk'yanets, E.A., 1998, *Ross. Khim. Zh.*, **XLII**, no. 5, 9.
3. Yakubovskaya, R.I., Kazachkina, N.I., Karmakova, T.A., *et al.*, 1998, *Ross. Khim. Zh.*, **XLII**, no. 5, 17.
4. Mironov, A.F., 1998, *Ross. Khim. Zh.*, **XLII**, no. 5, 23.
5. Stranadko, E.F., 1999, *Proc. 3rd All-Russia Symp. "Photodynamic Therapy"* (Moscow) (in Russian), p. 3.
6. Potter, W.R., Henderson, B.W., Bellnier, D.A., *et al.*, 1999, *Photochem. Photobiol.*, **70**, 781.
7. Robinson, D.J., de Bruijn, H.S., van der Veen, N., *et al.*, 1998, *Photochem. Photobiol.*, **67**, 140.
8. Fuchs, J. and Thiele, J., 1998, *Free Radic. Biol. Med.*, **24**, 835.
9. Hsi, R.A., Rosenthal, D.I., and Glatstein, E., 1999, *Drugs*, **57**, 725.
10. Kalka, K., Merk, H., and Mukhtar, H., 2000, *Am. Acad. Dermatol.*, **42**, 389; quiz 414–6.
11. Kulapaditharom, B. and Boonkitticharoen, V., 2000, *J. Med. Assoc. Thai*, **83**, 249.
12. Colussi, V.C., Feyes, D.K., and Mukhtar, H., 1998, *Skin Pharmacol. Appl. Skin Physiol.*, **11**, 336.
13. Cheong, W.F., Prahl, S.A., and Welch, A.J., 1990, *IEEE J. Quantum Electron.*, **26**, 2166.
14. Prahl, S.A. *et al.*, 1989, *SPIE Institute Series*, **IS5**, 102.
15. Flock, S.T., Patterson, M.S., Wilson, B.S., and Wyman, D.R., 1989, *IEEE Trans. Biomed. Eng.*, **36**, 1162.
16. Loschenov, V.B., Kuzin, M.I., Artjushenko, V.G., and Konov, V.I., 1989, *Proc. SPIE*, **1066**, 271.
17. Loschenov, V.B. and Steiner, R., 1993, *Proc. SPIE*, **2081**, 96.
18. Loschenov, V.B. and Steiner, R., 1994, *Proc. SPIE*, **2325**, 144.
19. Loschenov, V.B., Stratonnikov, A.A., Volkova, A.I., and Prokhorov, A.M., 1998, *Ross. Khim. Zh.*, **XLII**, no. 5, 50.
20. Stratonnikov, A.A., Loschenov, V.B., Duplik, A.Yu., and Konov, V.I., 1998, *Ross. Khim. Zh.*, **XLII**, no. 5, 63.
21. Kolesnikov, A.N., Agafonov, V.V., Belyaeva, L.A., *et al.*, 1999, *Proc. III All-Russia Symp. "Photodynamic Therapy"* (Moscow) (in Russian), p. 173.
22. Linkov, K.G., Kisselev, G.L., and Loschenov, V.B., 1996, *Proc. SPIE*, **2923**, 58.
23. Kiselev, G.L. and Loschenov, V.B., 1998, *Ross. Khim. Zh.*, **XLII**, no. 5, 53.
24. Duplik, A.Yu., Loschenov, V.B., and Stratonnikov, A.A., 1997, *Proc. II All-Russia Symp. with Int. Particip. "Photodynamic Therapy of Malignant Neoplasms"* (Moscow) (in Russian), p. 95.
25. Douplik, A.Yu., Loschenov, V.B., and Stratonnikov, A.A., 1997, *J. Int. Federation Med. Biol. Eng.*, **35**, 158.
26. Loschenov, V.B., Baryshev, M.V., Kuzin, M.I., *et al.*, 1991, *Proc. SPIE*, **1420**, 271.
27. Uspenskii, L.V., Dadvani, S.A., Chistov, L.V., *et al.*, 1999, *Khirurgiya*, no. 10.
28. Kharnas, S.S., Loschenov, V.B., Stratonnikov, A.A., *et al.*, 1994, *Proc. SPIE*, **2325**, 281.
29. Kharnas, S.S., Dadvani, S.A., Zavodnov, V.Ya., *et al.*, 1999, *Proc. III All-Russia Symp. "Photodynamic Therapy"* (Moscow) (in Russian), p. 96.
30. Stratonnikov, A.A., Edinac, N.E., Klimov, D.V., *et al.*, *Proc. SPIE*, **2924**, 49.
31. Shental', V.V., Paches, A.I., Loschenov, V.B., *et al.*, 1996, *Vestn. Ross. Akad. Med. Nauk*, p. 13.
32. Dadvani, S.A., Kharnas, S.S., Chilingaridi, K.E., *et al.*, 1999, *Khirurgiya*, no. 10, 75.
33. Vetshev, P.S., Chilingaridi, K.E., Ippolitov, L.I., *et al.*, 1999, *Problemy Endokrinologii*, no. 1, 17.
34. Babin, A.V., Loschenov, V.B., Korablin, S.N., and Ronzin, A.D., 1989, On the Methods of Early Oncological Diagnostics, *Methods of Prophylaxis and Treatment of Otorhinolaryngologic Organs* (Moscow: TsOLIUV) (in Russian), p. 29.
35. Kogan, E.A., Nevol'skikh, A.A., Zharkova, N.N., and Loschenov, V.B., 1993, *Arkhiv Patologii*, no. 6.

INVENTOR'S CERTIFICATES AND PATENTS

1. Loschenov, V.B., Stratonnikov, A.A., and Meerovich, G.A., 2000, Russian Federation Patent Application no. 20001064419.
2. Zhuravlev, D.A., Zhuravleva, V.P., Loschenov, V.B., and Stratonnikov, A.A., 1996, Russian Federation Patent Application no. 96107087.
3. Loschenov, V.B., Baryshev, M.V., Kuzin, M.I., *et al.*, 1991, Russian Federation Patent no. 2012243.
4. Kuzin, N.I., Zavodnov, V.Ya., Loschenov, V.B., *et al.*, 1989, USSR Inventor's Certificate no. 1506357.
5. Loschenov, V.B., Meerovich, G.A., and Lin'kov, K.G., 2000, Russian Federation Patent Application no. 2000112929.
6. Loschenov, V.B., Bashkatov, I.P., and Lin'kov, K.G., 1999, Russian Federation Patent Application no. 99113706.
7. Duplik, A.Yu., Loschenov, V.B., and Aleksandrov, M.T., 1994, Patent Application no. 94037116/25.
8. Loschenov, V.B., Duplik, A.Yu., Klimov, D.V., and Lin'kov, K.G., 1997, Patent Application no. 97106366.
9. Vorozhtsov, G.N., Dashkevich, S.N., Loschenov, V.B., and Luk'yanets, E.A., 1994, Patent no. RU 2071320 C1.
10. Loschenov, V.B., Kaliya, O.L., Luk'yanets, E.A., *et al.*, 1994, Russian Federation Patent no. 2113254.
11. Loschenov, V.B., Meerovich, G.A., Stratonnikov, A.A., *et al.*, 1996, Russian Federation Patent no. 2146159.
12. Kharnas, S.S., Kuzin, M.I., Kuzin, N.M., *et al.*, 1996, Russian Federation Patent no. 21446160.
13. Mitina, V.Kh., Klyashchitskii, B.A., Ponomarev, G.V., *et al.*, 1991, USSR Inventor's Certificate no. 1684289.
14. Vorozhtsov, G.N., Loschenov, V.B., Luk'yanets, E.A., *et al.*, 1997, Russian Federation Patent no. 2146144.
15. Loschenov, V.B., Duplik, A.Yu., Vorozhtsov, G.N., *et al.*, 1998, Russian Federation Patent Application no. 98113166/14 (014355).